Eng. Sci., 2022, **20**, 117–124

Engineered Science

DOI: https://dx.doi.org/10.30919/es8d760

Ferroelectric Relaxor Behavior and Dielectric Relaxation in Strontium Barium Niobate – A Lead-Free Relaxor Ceramic Material

Anamika Dwivedi,[1] K. N. Singh,[2,*] Milan Hait[3,*] and P. K. Bajpai[4]

Abstract

Various compositions of single-phase ceramics of Strontium barium niobate, $Sr_xBa_{1-x}Nb_2O_6$ (x=0.25, 0.50 abbreviated as SBN25 and SBN50) have been synthesized by standard solid-state reaction route by a precise control of cooling rate and optimizing the sintering temperatures. Material calcined at 1250 °C and sintered at 1300 °C is stabilized in pure phase with a tetragonal structure having density >95%. Lattice parameters for SBN25 (a= 12.467(4) Å, c=3.956(5) Å), and SBN50 (a= 12.435(2) Å, c= 3.945(7) Å). Both compositions show a relaxor type behavior with a diffuse phase transition. Modified Curie-Weiss law is used to fit the dielectric data. The dielectric relaxation obeys the Vogel–Fulcher relationship with a freezing temperature of 277.3 K for SBN25 and 278.4 K for SBN50. Significant dielectric dispersion is observed in the low frequency regime in both components of dielectric permittivity and a small dielectric relaxation peak is observed. This is associated with the defect related hopping process. The value of tilt parameter (α) in Cole-Cole analysis varies from 0.12 to 0.17 for SBN25 and 0.13 to 0.21 for SBN50 with increasing the temperature from 75 °C to 150 °C, indicates poly-dispersive nature of the dielectric relaxation. This material can be a good candidate for hologram and electro-optic data storage media.

Keywords: Ceramic; Dielectric relaxation; Relaxors; Vogel-Fulcher relation.
Received: 10 March 2022; Revised: 13 April 2022; Accepted: 19 July 2022.
Article type: Communication

1. Introduction:

Strontium barium niobate, (*i.e.*, $Sr_xBa_{1-x}Nb_2O_6$, SBN) have remarkable ferroelectric properties,[1] pyroelectric, linear electro-optic coefficients[2] and strong photorefractive effects[3] and have been widely applied in technological applications like storage media for holograms,[4] pyroelectric[5] and piezoelectric[6] applications, and electro-optic data storage.[7] SBN crystallizes in a tetragonal tungsten bronze structure, space group *P4bm*.[8] Ferroelectric SBN materials are stable since they contain no volatile element such as Pb[9,10] in the perovskite ferroelectrics. Although SBN single crystals are preferable for these applications, high cost and difficult fabrication limits their practical use.[11] SBN ceramics have the advantages of low cost, easy synthesis and are promising alternates for many applications. For optical and ferroelectric applications, high density and improved dielectric properties are greatly desired.[12-14] The use of solution based chemical synthesis methods ensures atomic level mixing of the reactants and hence can circumvent the high calcination temperature requirements associated with the conventional solid-state methods.

Unfortunately, the preparation of dense SBN ceramics through chemical synthesis methods gets complicated[15] by the moisture sensitivity and easy hydrolysis of the niobium sources.[16] Therefore, controlling the processing and parameters in the simple solid-state route to attain high density single phase seems to be the possible way. Although single crystals of SBN with varying composition have been used immensely,[17] there are limited applications because of the difficulty in fabrication and associated high cost. For optical applications, it is desirable that SBN should have a density

[1] *Department of Physics, YBN University, Ranchi, Jharkhand-834010, India.*
[2] *Department of Physics, OP Jindal University, Punjipathara Raigarh C.G. - 496109, India.*
[3] *Department of Chemistry, Dr. C. V. Raman University, Bilaspur C.G.-495113, India.*
[4] *Advance Research Laboratory, Department of Pure & Applied Physics, GGV, Bilaspur C.G.-495 009, India.*
**Email:* kn.singh@opju.ac.in (K. N. Singh); haitmilan@gmail.com (M. Hait)

near to theoretical one and uniform microstructure.[18]

In this study, solid solutions $Sr_xBa_{1-x}Nb_2O_6$ (x=0.25 and 0.50) abbreviated as SBN25 and SBN50 were synthesized in a simple solid-state reaction route. The ferroelectric relaxor behavior and dielectric relaxation in these important ceramics compositions keeping relatively low sintering temperature and higher density were studied. To the best of our knowledge, no such detailed report exists in literature.

2. Experimental Procedure

$Sr_xBa_{1-x}Nb_2O_6$ was synthesized by taking stoichiometric amount of high purity powder of $SrCO_3$ (Loba-99.9%), $BaCO_3$ (Loba-99.9%) and Nb_2O_5 (Loba-99.5%) using solid-state reaction route. The stoichiometric amounts of constituent's powders were wet mixed in acetone for 6 hours. The mixed powders were calcined at an optimum calcination temperature (1250 ºC) for 5 hours at the rate of 2 ºC/m. The calcined powders were structurally analyzed by X-ray diffraction technique using X-ray diffractometer (Rigaku, Miniflex). Fine calcined powders were pressed into cylindrical pellets of 10 mm diameter and 1-2 mm thickness under an iso-static pressure of 100 MPa. Polyvinyl alcohol (PVA) was used as a binder. The pellets were sintered at 1300 ºC, for 4 hours and cooled down to room temperature using a controlled cooling rate 2 ºC/min. The phase formation was identified using X-ray diffraction analysis again**.** To measure the dielectric properties, the sintered pallets were electroded with silver paste and heated at 500 ºC for 1 hour and cooled down up to room temperature before measurements. The dielectric data were taken in the temperature range (30-350 ºC) and at the heating rate of 2 ºC/min. The dielectric data were recorded using HIOKI 3532 LCR Hi TESTER impedance analyzer. Polarization vs. Electric field (P-E) data were recorded using P-E loop tracer (Marine India Pvt. Limited).

3. Results and Discussion

3.1 X-ray diffraction Study

Figure 1 shows the X-ray diffraction profile of $SrxBa_1$-xNb_2O_6 (x=0.25, 0.50 abbreviated as SBN25 and SBN50). The compositions have been confirmed as single phases with a tetragonal structure by indexing the observed XRD peaks using an XRD interpretation and indexing program POWD. The unit cell parameters were refined using the criteria that the sum of difference between the observed (d_{obs}) and the calculated (d_{cal}) interplaner spacing $\Sigma\Delta\delta = \Sigma (d_{obs}-d_{cal})$ is minimum. SBN is stabilized in a tetragonal structure with the lattice parameters of a=12.467(4) Å, c=3.956(5) Å, for SBN25 and a=12.435(2) Å, c=3.945(7) Å for SBN50. These values are very close to the earlier report (JCPDF-39-0265). The crystalline size was determined using Scherer formula and is 390Å (SBN25) and 440 Å (SBN50). A comparison of cell parameters shows that both a and c decreases for SBN50 in comparison to SBN25. SBN has a tungsten bronze type of structure,[19-21] with a unit cell formula of $(A_1)_2 (A_2)_4 C_4B_{10}O_{30}$, in which A_1, A_2, C and B cations are in the 15-, 12-, 9-, 6-coordinated sites, respectively. The Ba^{2+} ion predominantly occupies the 15- fold-coordinated sites as the radius of Ba^{2+} ion (1.74 Å) is substantially larger than that of the Sr^{2+} ion (1.44 Å). Therefore, the Sr^{2+} ion occupies either the A_2 or a combination of A_1- and A_2 - sites. As the Sr/Ba ratio is increased more Sr^{2+} occupy A_2- sites. Considering the larger ionic radius of Ba^{2+} than Sr^{2+}, it can be understood that the decrease of unit cell parameters of SBN50 reflects that more Sr^{2+} and less Ba^{2+} are absorbed into SBN solid solution.

The formation of pure TTB phase in both compositions (x= 0.25, 0.50) at a relatively lower sintering temperature (*i.e.*, 1300 ºC) and a higher densification (>95% density) is achieved in the present studies in comparison to 1350 ºC (92% density) as reported by Qu *et al*.[22] or 1400 ºC as reported by Ho *et al*.[23] is significant as it may reduce the problem of abnormal grain growth, occurring due to high sintering temperatures. It is noted that electrical and optical properties are deteriorated due to the abnormal grain growth.

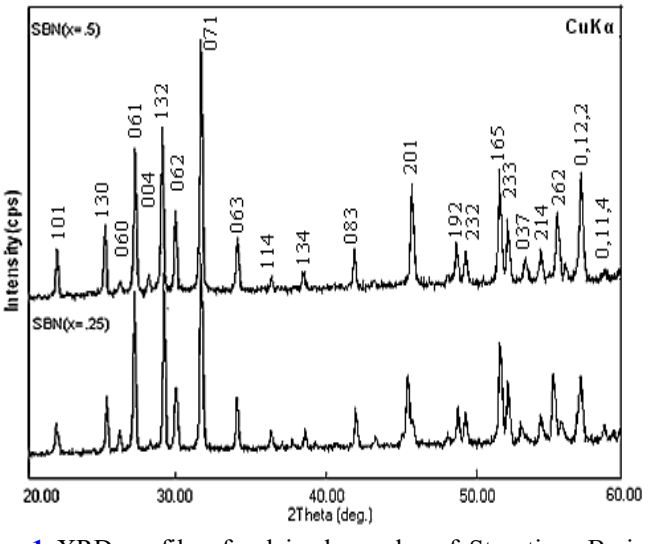

Fig. 1 XRD profile of calcined powder of Strontium Barium niobate (SBN) at room temperature.

3.2 Dielectric Study

Figure 2(a) and 2(b) shows the temperature dependence of dielectric constants (ε') for both solid solutions, which exhibit a broad maximum with a shift towards higher temperature for raising frequencies, whereas its maximum value (ε'_m) decreases. A frequency dispersion takes place at temperature (T) < Maximum temperature (T_m). The temperature and frequency dependence of dielectric loss (tanδ) is plotted in Figs. 3(a) and 3(b). A shift of the temperature T'_m of tanδ to higher values for raising frequencies is observed. Further T_m of (ε'_m) and T'_m of (tanδ) do not coincide at a given frequency. The transition temperature decreases with increase in Sr content in SBN. The maximum relative permittivity (ε'_m) as well as its corresponding temperature (T_m) is given in Table 1. Hence, these results suggest that the dielectric polarization has a relaxation-type behavior and composition to be of relaxor

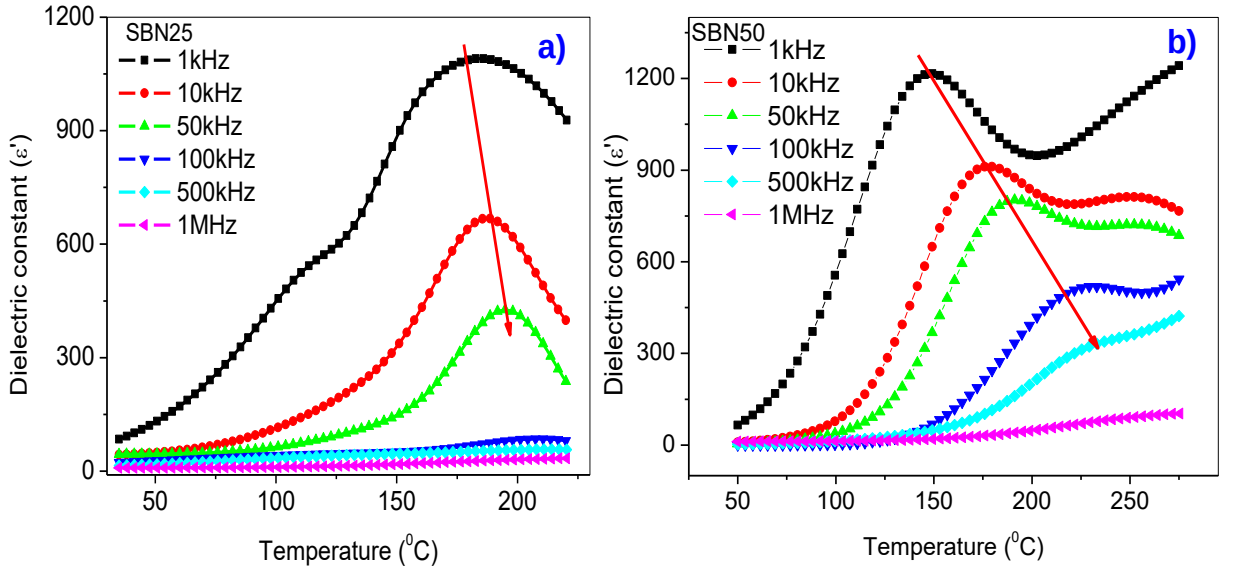

Fig. 2 Temperature dependence of dielectric constant of a) SBN25 and b) SBN50.

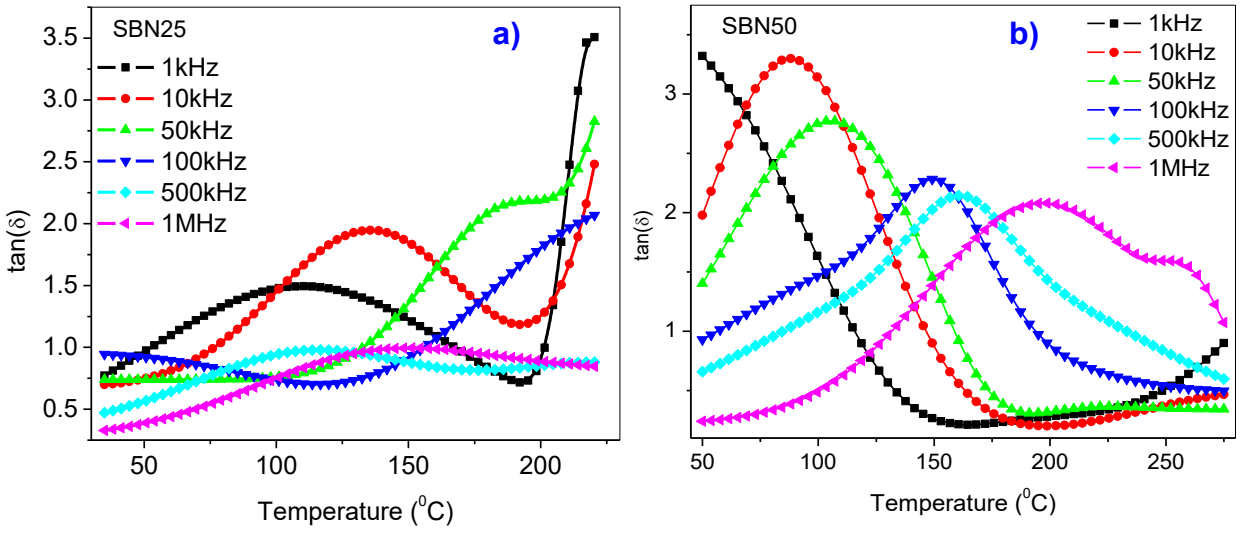

Fig. 3 Temperature dependence of dielectric loss of a) SBN25 and b) SBN50.

Table 1. Maximum temperature (T_m) and peak dielectric constant values (ε'_m) at representative frequencies in different compositions of SBN.

Frequency	SBN25		SBN50	
(kHz)	T_m(°C)	ε'_m	T_m(°C)	ε'_m
1	178	1090	148	1216
10	188	668	176	911
50	195	427	190	802
100	210	169	220	507

type. However, significant frequency dispersion is seen in ε' for temperatures $T > T_m$ also, especially in SBN50, unlike for the classical relaxor materials. This may be associated with the increased distortion in SBN ceramics as is well known that with increasing the Sr/Ba ratio, the distortion increases.

To analyze the observed diffuse phase transition characteristics further, frequency dispersion (ΔT_m) and the diffusivity (γ) are used to reflect the relaxor behavior of the studied ceramics. It is well known that the dielectric constant for normal ferroelectrics above the Curie temperature follows the Curie–Weiss law[24] as described by Equation (1):

$$\frac{1}{\varepsilon'} = \frac{(T-\Theta)}{C} \quad (T > T_c) \tag{1}$$

where, Θ is the Curie temperature, and C is the Curie constant. The Curie–Weiss plot between (1/ε' vs. temperature) gives a straight line with a slope of (1/C) and the X-axis intercept at

Θ. Figs. 4(a) and 4(b) shows the Curie–Weiss plot for SBN25 and SBN50 at 1 kHz. The degree of deviation from the Curie–Weiss behavior could be given by ΔT_m, which is determined by Equation (2):

$$\Delta T_m = T_B - T_m \quad (2)$$

where, T_B represents the temperature from which ε' starts to deviate from the Curie–Weiss law, and T_m denotes the temperature of dielectric permittivity maximum (ε'_m). The difference between two temperatures, (T_B- T_m), could be used to characterize the diffuseness of phase transition.[25] At 1 kHz, ΔT_m = 22 ºC/18 ºC for SBN25/SBN50. The Curie temperature Θ, the Burn temperature, T_B and the temperature difference (T_B - T_m) are summarized in Table 2 for both compositions. Another parameter $\Delta T_{m\,(relax)}$ is used to characterize the degree of relaxation behavior in the frequency range of 1 kHz to 100 kHz, as described[26] in Equation (3):

$$\Delta T_{m\,(relax)} = T_{m\,(100\ kHz)} - T_{m\,(1\ kHz)} \quad (3)$$

where, $\Delta T_{m\,(relax)}$ is obtained from the dielectric measurements (Table 1) and is approximately 32 ºC (SBN25) and 72 ºC (SBN50).

The dielectric behavior of a relaxor ferroelectric could be described by a modified Curie–Weiss law[27] as given by Equation (4):

$$\frac{1}{\varepsilon'} - \frac{1}{\varepsilon'_m} = \frac{(T-T_m)^{\gamma}}{C'} \quad (4)$$

where, γ and C' are measured to be constants, the value of γ lies between 1 and 2. The parameter γ gives information on the phase transition character; γ = 1 represents classical ferroelectric phase transition where normal Curie-Weiss law is followed and γ = 2 gives the quadratic dependence which describes a complete diffuse phase transition. Figs. 5(a) and 5(b) shows the plot of log ($1/\varepsilon - 1/\varepsilon_m$) vs. log ($T-T_m$) at 1kHz for SBN25 and SBN50 respectively. A linear relationship is obvious from the plot. The value of γ estimated from the slope of the graphs is 1.25, 1.35 for SBN25 and SBN50 respectively, indicating that the materials have diffuse phase transition characteristics.

The observed broadness or diffuseness occurs mainly because of the compositional fluctuations and/ or due to structural disorder in the lattice.[28] This may be correlated with the prevailing disorder at A-site due to the two cations (Ba^{2+} and Sr^{2+}) competing at this site. Thus, the dielectric polarization may be similar to that observed in the dipolar glasses. In analogy with spin glasses, the dynamic susceptibility behavior in disordered ferroelectrics is supposed to be associated with a broad spectrum of relaxation time. Therefore, the Debye model, which is based on the single relaxation time, fails when employed for a system with a distributed relaxation time.

Figure. 6(a) and 6(b) shows the curve of log (ω) vs. $1/T_m$ for SBN25 and SBN50 respectively. A nonlinear behavior is observed indicating that the data do not obey the simple Debye equation. In order to analyze relaxor characteristics of SBN ceramics, the experimental curve (Fig. 6) was fitted using Vogel–Fulcher relation[29,30] as written in Equation (5):

$$\omega = \omega_o \exp\left[\frac{-E_a}{k_B(T_m - T_f)}\right] \quad (5)$$

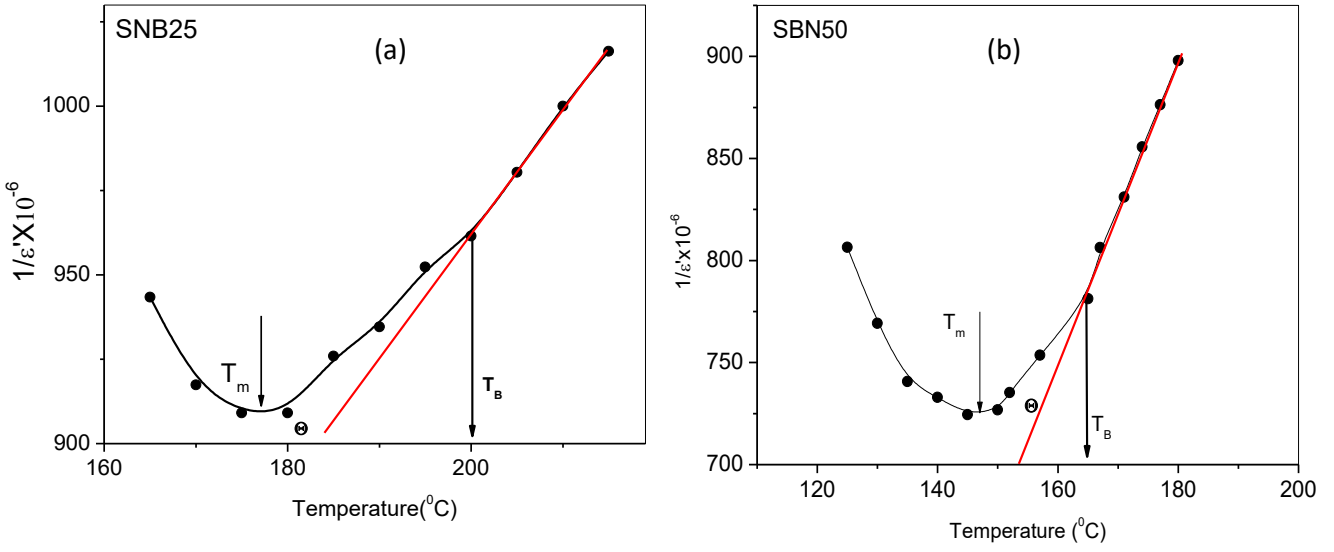

Fig. 4 (a) Temperature dependence of the reciprocal dielectric constant (1/ε′) for SBN25 fitted with Curie–Weiss law at 1 kHz, (b) Temperature dependence of the reciprocal dielectric constant (1/ε′) for SBN50 fitted with Curie–Weiss law at 1 kHz.

Table 2. Characteristic parameters determined and calculated from ε′(T) measurements.

Sample	Frequency(KHz)	T_m(ºC)	Θ(ºC)	T_B(ºC)	$\Delta T_m=T_B-T_m$
SBN25	1	178	184	200	22
SBN50	1	148	154	166	18

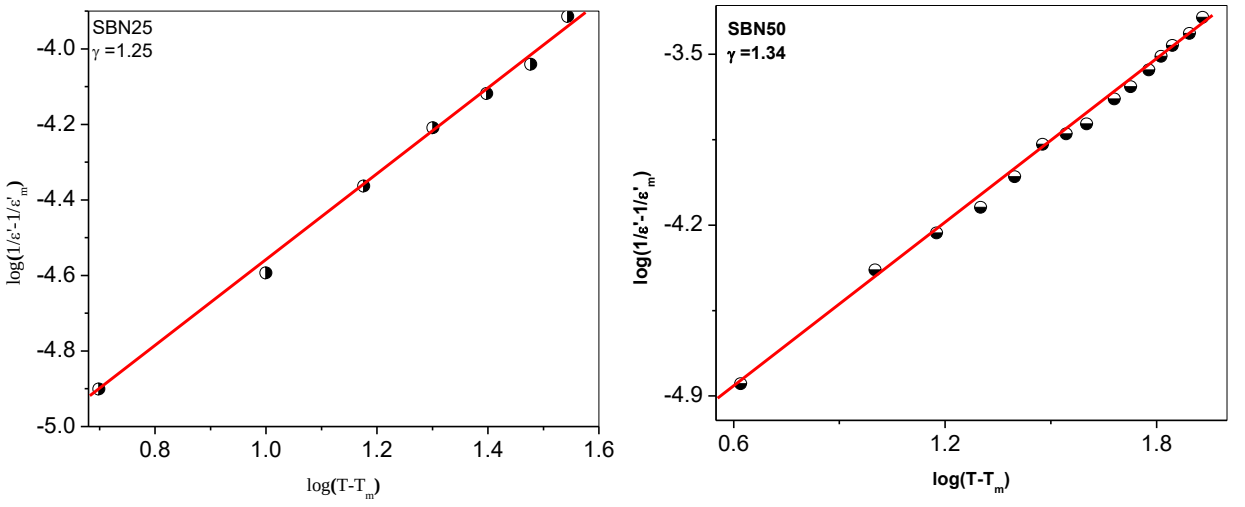

Fig. 5 (a) log (1/ε -1/εm) as function of log(T-Tm) for SBN25 at 1 kHz (b) log (1/ε -1/εm) as function of log(T-Tm) for SBN50 at 1 kHz.

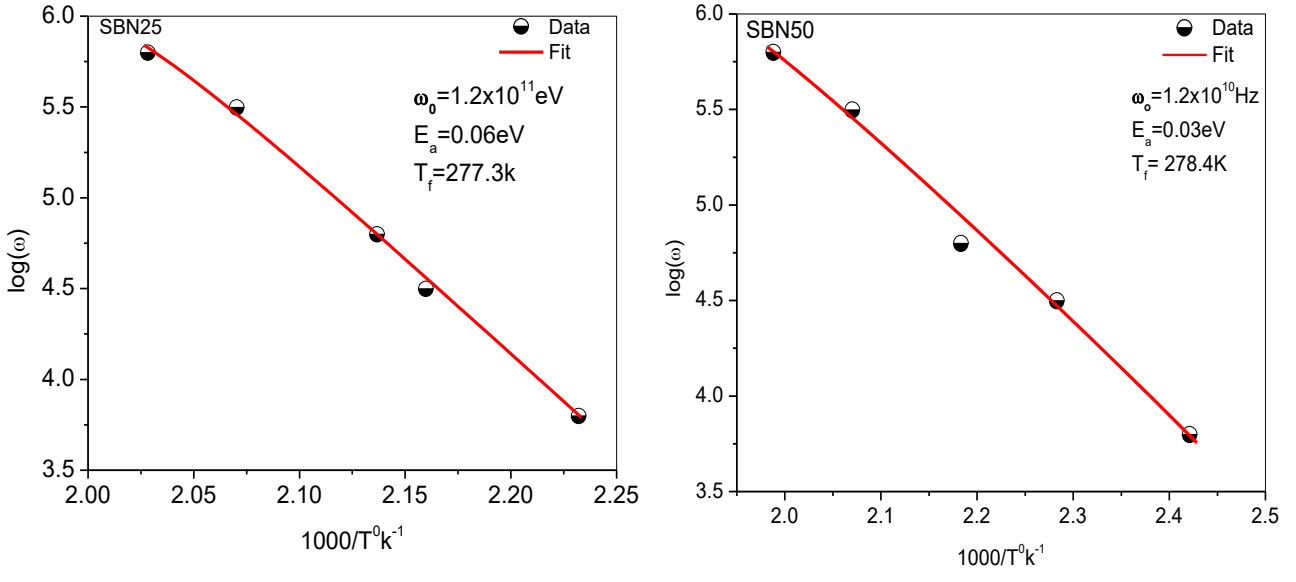

Fig. 6 (a) log(ω) versus l/Tm plot for SBN25. The solid line represents the fitting to Vogel-Fulcher relationship, (b) log(ω) versus l/T_m plot for SBN50. The solid line represents the fitting to Vogel–Fulcher relationship.

where, T_f is considered as the temperature, at which the dynamic reorientation of distorted [NbO_6] clusters leads to polarization in the lattice. Figs. 6(a) and 6(b) exhibits the Vogel–Fulcher plot for the SBN compositions. The fitting parameters used in the Vogel–Fulcher equation are summarized in Table 3.

The poly-dispersive nature of dielectric relaxation is demonstrated through Cole-Cole plots. For a mono-dispersive Debye process, one expects semicircular plots with the center located on the ε'-axis, whereas for distributed (poly-dispersive) relaxation, these plots are close to circular arcs with end-points on the real axis and the center below the axis. In the Cole-Cole formalism, the complex dielectric constant is then described by Equation (6):

$$\varepsilon^* = \varepsilon_\infty + (\varepsilon_s - \varepsilon_\infty)/1 + (j\omega\tau)^{1-\alpha} \quad (6)$$

where, ε_s and ε_∞ are the low and high frequency values of ε', tilt parameter (α) is a measure of the distribution of relaxation times, $\tau = \omega^{-1}$. The parameter, α can be determined from the location of the center of the Cole-Cole circles,[31] of which only an arc lies above the ε' axis. Such plots are shown in Figs. 7(a) and 7(b) for SBN25 and SBN50 respectively. It is evident from these plots that the relaxation process differs from the Debye process (for which α=0).[28] The measured dielectric data are fitted in Equation (6) and the average relaxation time (τ) and tilt parameter (α) are obtained and given in Table 4. The parameter α, representing the angle subtended by the radius of the circle with the real axis passing through the origin of ε'–axis, shows a consistent increase with increasing temperature (Table 4). This suggests the temperature dependent relaxation process. Thus the Cole-Cole plots indicate the temperature dependent polydispersive nature of the dielectric relaxation in SBN.

Table 3. Vogel–Fulcher law fitting parameters; the pre-exponential factor ω_o, activation energy E_a and freezing temperature T_f for different compositions of SBN.

Sample	ω_o(Hz)	E_a(eV)	T_f(K)
SBN25	1.2×10^{11}	0.06	277.3
SBN50	1.2×10^{10}	0.03	278.4

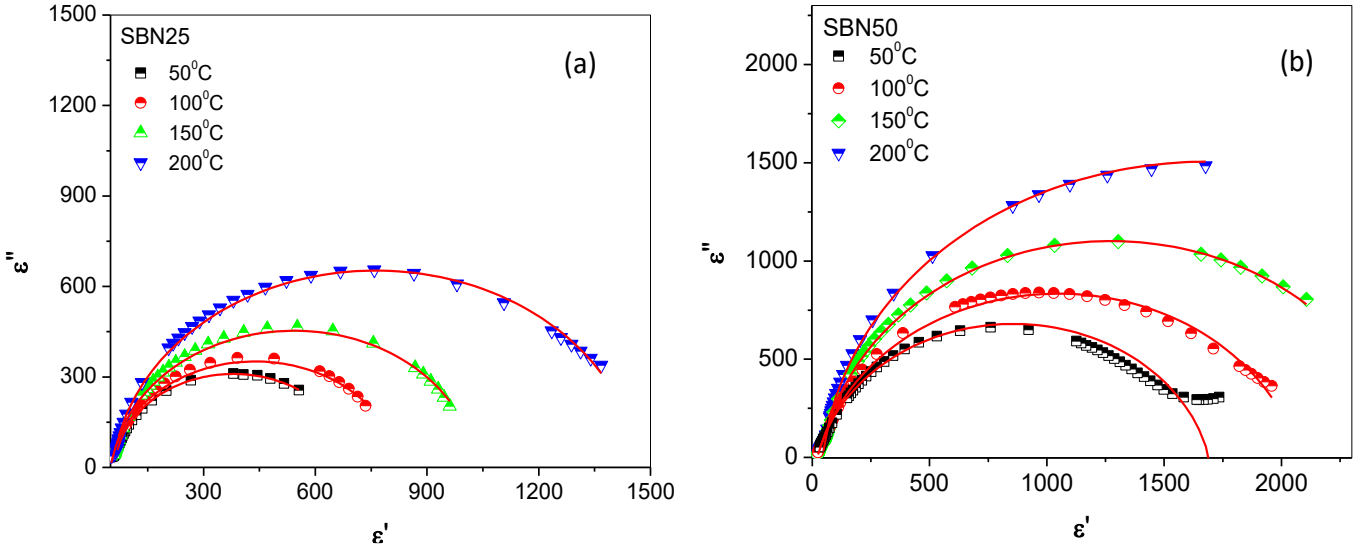

Fig. 7 (a) Cole-Cole plots between ε′ and ε" for SBN25 at some representative temperatures, (b) Cole-Cole plots between ε′ and ε" for SBN50 at some representative temperatures.

Table 4. Average relaxation time (τ) and tilt parameter (α) obtained from the Cole- Cole expression for different compositions of SBN ceramics.

Temperature (°C)	SBN25		SBN50	
	τ	α	τ	α
75	1.2×10^{-6}	0.12	3.6×10^{-6}	0.13
100	8.0×10^{-6}	0.13	7.1×10^{-6}	0.15
125	4.0×10^{-5}	0.14	2.5×10^{-5}	0.19
150	8.0×10^{-5}	0.17	6.0×10^{-5}	0.21

4. Conclusions

SBN ceramic compositions calcined at 1250 °C and sintered at 1300 °C are stabilized in the phase with a pure tetragonal structure having lattice parameters of (a = 12.4674 Å, c = 3.9565 Å), for SBN25 and (a = 12.4352Å, c= 3.9457Å) for SBN50. The phase pure ceramics are obtained at relatively low sintering temperatures and with higher density (>95%) than that of the theoretical value. The modified Curie law is used to fit the experimental data indicating that the compositions have diffuse phase transition characteristics with γ = 1.25 and 1.35 for SBN25 and SBN50 respectively. The values of the parameters T_m = 178 and 148 °C, T_B = 200 and 166 °C and ΔT_m (=T_B - T_m) 22 and 18 °C (for SBN25 and SBN50 respectively) obtained as a characteristic diffuseness of phase transition are smaller to those obtained for classical relaxors. The Vogel–Fulcher relationship is found to be valid and is used to obtain characteristic parameters of diffuse phase transitions *i.e.*, relaxation frequency, activation energy, E_a and freezing temperature T_f. It shows that with increasing the Sr^{2+} content, the relaxation slows down (ω_o changes from 1.2×10^{11} Hz to 1.2×10^{10} Hz) with lower activation energy E_a (0.06 eV→0.03 eV) and freezing temperature (T_f) slightly increasing (277.3 K→278.4 K). The low frequency dielectric dispersion is observed and is associated with the defect related hopping process. The Cole-Cole plots of dielectric constant indicate the polydispersive nature of the dielectric relaxation. As a result, this ceramic composite material is suitable for use in a wide variety of contexts, including pyroelectricity and piezoelectricity.

Conflict of Interest

The authors declare no conflict of interest.

Supporting information

Not applicable.

References

[1] A. M. Glass, Ferroelectric $Sr_{1-x}Ba_xNb_2O_6$ as a Fast and Sensitive Detector of Infraed Radiation, *Applied Physics Letters*, 1968, **13**, 147-149, doi: 10.1063/1.1652547.

[2] S. Sakamoto, T. Yazzki, Anomalous Electro-optic Properties of Ferroelectric Strontium Barium Niobate and Their Device Applications, *Applied Physics Letters*, 1973, **22**, 429-431, doi: 10.1063/1.1654700.
[3] W. H. Liu, Y. S. Qiu, H. J. Zhang, J. H. Dai, P. Y. Wang, L. Y. Xu, Energy Transfer in $Sr_{0.56}Ba_{0.44}Nb_2O_6$: Ce AT 633 nm, *Optics Communications*, 1987, **64**, 81-84, doi: 10.1016/0030-4018(87)90374-9.
[4] T. Kume, K. Nonaka, M. Yamamoto, Wavelength-Multiplexed Holographic Recording in Cerium Doped Strontium Barium Niobate by Using Tunable Laser Diode, *Japanese Journal of Applied Physics*, 1996, **35**, 448, doi: 10.1143/JJAP.35.448.
[5] S. T. Liu, R. B. Maciolek, Rare-earth-modified $Sr_{0.5}Ba_{0.5}Nb_2O_6$, ferroelectric crystals and their applications as infrared detectors, *Journal of Electronic Materials*, 1975, **4**, 91-100, doi: 10.1007/bf02657838.
[6] T. T. Fang, E. Chen, W. J. Lee, On the discontinuous grain growth of $Sr_xBa_{1-x}Nb_2O_6$ ceramics, *Journal of the European Ceramic Society*, 2000, **20**, 527-530, doi: 10.1016/S0955-2219(99)00178-8.
[7] Y. S. Yang, M. K. Rhy, H. J. Joo, S. H. Lee, S. J. Lee K. Y. Kang, M. S. Jang, Ferroelectricity and electronic defect characteristics of c-oriented thin films deposited on Si substrates, *Applied Physics Letters*, 2000, **76**, 3472-3474, doi: 10.1063/1.126681.
[8] P. B. Jamieson, S. C. Abrahams, J. L. Bernstein, Ferroelectric Tungsten Bronze-Type Crystal Structures. II. Barium Sodium Niobate $Ba_{(4+x)}Na_{(2-2x)}Nb_{10}O_{30}$, *Journal of Chemistry and Physics*, 1969, **50**, 4352-4363, doi: 10.1063/1.1668176.
[9] H. F. Cheng, M. H. Yeh, K. S. Liu, I. N. Lin, Characteristics of $BaTiO_3$ films prepared by pulsed laser deposition, *Japanese Journal of Applied Physics*, 1993, **32**, 5656, doi: 10.1143/JJAP.32.5656.
[10] H. F. Cheng, G. S. Chiou, K. S. Liu, I. N. Lin, Ferroelectric properties of $(Sr_{0.5}Ba_{0.5})Nb_2O_6$ thin films synthesized by pulsed laser deposition, *Applied Surface Science*, 1997, **113-114**, 217-221, doi: 10.1016/s0169-4332(96)00794-5.
[11] J. T. Shiue, T. T. Fang, The sintering behavior of CeO2-doped strontium barium niobate ceramics, *Journal of the European Ceramic Society*, 2002, **22**, 1705-1709, doi: 10.1016/S0955-2219(01)00476-9.
[12] K. Nagata, Y. Yamamoto, H. Igarashi, K. Okazaki, Properties of the hot-pressed strontium barium niobate ceramics, *Ferroelectrics*, 1981, **38**, 853-856, doi: 10.1080/00150198108209556.
[13] S. I. Lee, W. K. Choo, Modified ferroelectric high density strontium barium niobate ceramics for pyroelectric applications, *Ferroelectrics*, 1988, **87**, 209-212, doi: 10.1080/00150198808201383.
[14] N. S. VanDamme, A. E. Sutherland, L. Jones, K. Bridger, S. R. Winzer, Fabrication of optically transparent and electrooptic strontium Barium niobate ceramics, *Journal of the American Ceramic Society*, 1991, **74**, 1785-1792, doi: 10.1111/j.1151-2916.1991.tb07789.x.
[15] R. N. Das, P. Pramanik, Chemical synthesis of fine powder of lead magnesium niobate using niobium tartarate complex, *Materials Letters*, 2000, **46**, 7-14, doi: 10.1016/s0167-577x(00)00134-8.
[16] J. H. Choy, J. S. Yoo, S. G. Kang, S. T. Hong, D. G. Kim, Ultra-fine (PMN) powder synthesized from metal-citrate gel by thermal shock method, *Materials Research Bulletin*, 1990, **25**, 283-291, doi: 10.1016/0025-5408(90)90099-n.
[17] M. M. A. Sekar, A. Halliyal, Low-Temperature Synthesis, Characterization, and Properties of Lead-Based Ferroelectric Niobates, *Journal of the American Ceramic Society*, 1998, **81**, 380-388, doi: 10.1111/j.1151-2916.1998.tb02344.x.
[18] Y. Narender and G. L. Messing, Kinetic analysis of combustion synthesis of lead magnesium niobate from metal carboxylate gels, *Journal of the American Ceramic Society*, 1997, **80**, 915-924, doi: 10.1111/j.1151-2916.1997.tb02922.x.
[19] M. H. Francombe, The relation between structure and ferroelectricity in lead Barium and Barium strontium niobates, *Acta Crystallographica*, 1960, **13**, 131-140, doi: 10.1107/s0365110x60000285.
[20] S. K. Ye, J. Y. H. Fuh, L. Lu, Structure and electrical properties of< 001> textured $(Ba_{0.85}Ca_{0.15})(Ti_{0.9}Zr_{0.1})O_3$ lead-free piezoelectric ceramics, Piezoelectric ceramics. *London: Academic Press*, 1971.
[21] A. M. Glass, Investigation of the Electrical Properties of Sr1−xBaxNb2O6 with Special Reference to Pyroelectric Detection, *Journal of Applied Physics*, 1969, **40**, 4699-4713, doi: 10.1063/1.1657277.
[22] M. T. M. Ho, C. L. Mak, K. H. Wong, Study of the formation mechanism of sol-gel derived sen powders using raman spectroscopy and X-ray diffractometry, *Ferroelectrics*, 1999, **231**, 255-260, doi: 10.1080/00150199908014540.
[23] Y. Q. Qu, A. D. Li, Q. Y. Shao, Y. F. Tang, D. Wu, C. L. Mak, K. H. Wong, N. B. Ming, Structure and electrical properties of strontium Barium niobate ceramics, *Materials Research Bulletin*, 2002, **37**, 503-513, doi: 10.1016/s0025-5408(02)00676-1.
[24] L. Zhou, P. M. Vilarinho, J. L. Baptista, The characteristics of the diffuse phase transition in Mn doped relaxor ceramics, *Journal of Applied Physics*, 1999, **85**, 2312-2317, doi: 10.1063/1.369543.
[25] L. Zhou, P. M. Vilarinho, J. L. Baptista, Relaxor behavior of $(Sr_{0.8}Ba_{0.2})$ TiO_3 ceramic solid solution doped with bismuth, *Journal of Electroceramics*, 2000, **5**, 191-199, doi: 10.1023/A:1026586226361.
[26] C. Ang, Z. Jing, and Z. Yu, Ferroelectric relaxor Ba (Ti, Ce) O_3, *Journal of Physics: Condensed Matter*, 2002, **14**, 8901, doi: 10.1088/0953-8984/14/38/313.
[27] G. S. Fulcher, Analysis of recent measurements of the viscosity of glasses, *Journal of the American Ceramic Society*, 1925, **8**, 339-355, doi: 10.1111/j.1151-2916.1925.tb16731.x.
[28] P. K. Bajpai, M. Pastor, K. N. Singh, Relaxor behavior and dielectric relaxation in $Pb(Ba_{1/3}Nb_{2/3})O_3$: A phase pure new relaxor material, *Journal of Applied Physics*, 2011, **109**, 014114, doi: 10.1063/1.3528219.

[29] Y. Guo, K. Kakimoto, H. Ohsato, Ferroelectric-relaxor behavior of $(Na_{0.5}K_{0.5})$ NbO_3-based ceramics, *Journal of Physics and Chemistry of Solids*, 2004, **65**, 1831-1835, doi: 10.1016/j.jpcs.2004.06.018.
[30] S. K. Rout, T. Badapanda, E. Sinha, S. Panigrahi, P. K. Barhai, T. P. Sinha, Dielectric and phase transition of $BaTi_{0.6}Zr_{0.4}O_3$ ceramics prepared by a soft chemical route, *Applied Physics A*, 2008, **91**, 101-106, doi: 10.1007/s00339-007-4366-1.
[31] K.S. Cole, R.H. Cole, Dispersion and absorption in dielectrics, *Journal of chemistry and physics*, 1941, **9**, 341, doi: 10.1063/1.1750906.

Author Information

Anamika Dwivedi *obtained her Bachelor of Science degree in 2015 from Dr. C. V. Raman University in Bilaspur, Chhattisgarh, India. In 2017, she earned her Master of Science degree from the same university and was awarded a gold medal for her studies. She is currently a PhD scholar in the Department of Physics, YBN University, Ranchi, India, and is working with Dr. P. K. Bajpai's group. Her current research focuses on ferroelectrics, multiferroics, thin films, crystal growth, and other areas of material science.*

Dr. K. N. Singh *is an Associate Professor in the Department of Physics at O. P. Jindal University in Punjipathara, Raigarh, Chhattisgarh, India. In 2010, he earned his doctorate in Material Science from the Advanced Material Research Laboratory, Department of Pure & Applied Physics, Guru Ghasidas Vishwavidyalaya (A Central University), Bilaspur, Chhattisgarh, India. His research concentrated on the development and characterization of some lead-based and lead-free relaxor materials using impedance spectroscopy. Areas of research interest include ferroelectrics, multiferroics, thin films, and crystal growth.*

Dr. Milan Hait*, FICS, is an Assistant Professor in Chemistry at the Department of Chemistry, Dr. C. V. Raman University, Bilaspur, Chhattisgarh, India. He achieved his M.Sc. in chemistry in 2006 from the Guru Ghasidas University, Bilaspur (C.G.), India; he obtained his M.Phil degree in 2011 at Dr. C. V. Raman University, and then completed his PhD degree at the same university in 2015. He joined the faculty of Dr. C. V. Raman University as an Assistant Professor in September 2011. His current research interests are focused on: synthesis of biologically active molecules; identification and validation of new bio-molecular targets for various therapeutic areas; elucidation of the effective components of herbal medicines; biosynthesis of natural products; analysis of water quality; bio-adsorbents; molecular recognition; and bio/chemosensors.*

Dr. P. K. Bajpai*, Professor and Dean, School of Physical Sciences, Guru Ghasidas Vishwavidyalaya, Bilaspur, India. He obtained his doctorate from the physics department of North-Eastern Hill University in 1988. He worked for North Eastern Hill University, 1988-1996; and Guru Ghasidas University, 1996-till date. He is the Centre In-charge, National Centre for Accelerator Based Research, Department of Pure & Applied Physics, GGV, Bilaspur (C.G.), India. 3.0 MV Pelletron accelerator-based research centre, supported by DAE under BRNS, a Flagship initiative for accelerator-based interdisciplinary research. He is a Fellow of the International Academy of Physical Sciences, the American Nano Society, and the New York Academy of Sciences. His current research focuses on developing nanostructures on ferroelectric surfaces via SHI irradiation and modelling; dye-protein interactions for plastic microfibers; charge-compensated sensor ceramics; new lead and non-lead Relaxor ferroelectrics for MLCs; structure-phase transition in ferroelectric single crystals; material characterization for pyroelectric detectors; D-Ram & communicational devices; system analysis & filter design.*

